Dichotomous regulation of group 3 innate lymphoid cells by nongastric *Helicobacter* species

John W. Bostick[a,b], Yetao Wang[c,1], Zeli Shen[d], Yong Ge[a], Jeffrey Brown[e], Zong-ming E. Chen[f], Mansour Mohamadzadeh[a], James G. Fox[d,g], and Liang Zhou[a,2]

[a]Department of Infectious Diseases and Immunology, College of Veterinary Medicine, University of Florida, Gainesville, FL 32608; [b]Department of Chemical and Biological Engineering, Northwestern University, Evanston, IL 60208; [c]Department of Microbiology-Immunology, Feinberg School of Medicine, Northwestern University, Chicago, IL 60611; [d]Division of Comparative Medicine, Massachusetts Institute of Technology, Cambridge, MA 02139; [e]Department of Pediatrics, Division of Gastroenterology, Hepatology and Nutrition, Northwestern Feinberg School of Medicine, Ann & Robert H. Lurie Children's Hospital of Chicago, Chicago, IL 60611; [f]Department of Laboratory Medicine and Pathology, Mayo Clinic, Rochester, MN 55905; and [g]Department of Biological Engineering, Massachusetts Institute of Technology, Cambridge, MA 02139

Edited by David Artis, Weill Cornell Medical College, New York, NY, and accepted by Editorial Board Member Ruslan Medzhitov October 24, 2019 (received for review May 10, 2019)

Intestinal innate lymphoid cells (ILCs) contribute to the protective immunity and homeostasis of the gut, and the microbiota are critically involved in shaping ILC function. However, the role of the gut microbiota in regulating ILC development and maintenance still remains elusive. Here, we identified opposing effects on ILCs by two *Helicobacter* species, *Helicobacter apodemus* and *Helicobacter typhlonius*, isolated from immunocompromised mice. We demonstrated that the introduction of both *Helicobacter* species activated ILCs and induced gut inflammation; however, these *Helicobacter* species negatively regulated RORγt$^+$ group 3 ILCs (ILC3s), especially T-bet$^+$ ILC3s, and diminished their proliferative capacity. Thus, these findings underscore a previously unknown dichotomous regulation of ILC3s by *Helicobacter* species, and may serve as a model for further investigations to elucidate the host–microbe interactions that critically sustain the maintenance of intestinal ILC3s.

host–microbiome | ILC | *Helicobacter* | inflammation

Innate lymphoid cells (ILCs) are a subset of immune cells that are involved in the protection and homeostasis of mucosal and barrier tissues, but sometimes play pathogenic roles in disease (1, 2). ILCs can be divided into "helper-like" (group 1, 2, and 3 ILCs: ILC1, ILC2, and ILC3) and cytotoxic (natural killer: NK) ILCs. Both helper-like and cytotoxic ILCs express molecules (e.g., cytokines) that promote immunity, but NK cells have the additional capacity to kill other cells through the expression of cytotoxic molecules. Helper-like ILCs are mainly tissue resident at steady state (with the exception of a population of circulating ILC1), but enter circulation under chronic inflammatory conditions in both mice and humans (3–6). In contrast, NK cells are readily found in the circulation, but may also establish tissue residency (3). P-selectin glycoprotein ligand-1 (PSGL-1; *Selplg*) is expressed on the surface of immune cells and plays a key functional role in their recruitment from the circulation to areas of inflammation (7) and homing to secondary lymphoid tissues during steady state (8). The critical signals involved in driving the movement of ILCs between tissue residence and circulation remain to be determined. Specifically, whether PSGL-1 plays an important role in ILC function in the intestine has not been clearly defined.

In this study, we sought to determine the role of PSGL-1 in ILC residence in and circulation from the intestine by crossing PSGL-1 knockout mice with Rag1 knockout mice that lack T and B cells but retain ILCs. Strikingly, we found that *Rag1*$^{-/-}$*Selplg*$^{-/-}$ double knockout mice had severely reduced ILC3s in the colon. The phenotype was transferable to *Rag1*$^{-/-}$ mice after cohousing and was not dependent on PSGL-1 deficiency. Moreover, the loss of ILC3s was ameliorated by antibiotics treatment, implicating the microbiota as the major driving factor for the immune phenotypes. Using selective antibiotics and 16S rRNA gene sequencing, we identified that the acquisition and overgrowth of pathobionts, *Helicobacter typhlonius* and *Helicobacter apodemus*, contributed to a decrease in the proliferative capacity and subsequent loss of ILC3s in the colon.

In human and murine studies, *Helicobacter* spp. induce pathogenic responses in their hosts, especially under conditions of compromised immunity (9, 10). Gastric *Helicobacter* spp., such as *Helicobacter pylori*, are clinically significant inducers of peptic ulcers, gastric adenocarcinoma, and mucosa-associated lymphoid tissue (MALT) lymphoma (11). Nongastric *Helicobacter* spp., which populate the intestine rather than the stomach, can induce strong T cell responses and promote the activation and proliferation of both effector and regulatory T cells (12, 13). Previous studies demonstrated that ILCs participate in the pathogenic response to *Helicobacter* spp., by promoting the production of proinflammatory cytokines (12, 14–17). Here, we demonstrate *Helicobacter*-induced suppression of ILC3s, uncovering a previously unrecognized negative regulation of ILCs by nongastric *Helicobacter* spp.

Results

Rag1$^{-/-}$_Selplg_$^{-/-}$ Mice Have Reduced Numbers of ILC3s in the Colon. To investigate the role of PSGL-1 in ILC maintenance and/or function in the gut, we bred *Rag1*-deficient mice with *Selplg*-deficient

Significance

Innate lymphoid cells (ILCs) in the intestine maintain both defense against pathogens and homeostasis of intestinal tissue, which is exposed to environmental influences, including microbes and ingested foods. We identified a pair of *Helicobacter* species that activate ILCs but negatively regulate proliferation of group 3 RORγt$^+$ ILCs (ILC3s) that are important for host immunity and inflammation. This opens the door for future investigations that explore the molecular factors produced by microbes that may influence the maintenance of ILC3s in the intestine.

Author contributions: J.W.B. and L.Z. designed research; J.W.B., Y.W., Z.S., Y.G., Z.-m.E.C., M.M., and J.G.F. performed research; Z.S., J.B., M.M., and J.G.F. contributed new reagents/analytic tools; J.W.B., Z.-m.E.C., and L.Z. analyzed data; and J.W.B. and L.Z. wrote the paper.

The authors declare no competing interest.

This article is a PNAS Direct Submission. D.A. is a guest editor invited by the Editorial Board.

Data deposition: The data reported in this paper have been deposited in the Gene Expression Omnibus (GEO) database, www.ncbi.nlm.nih.gov/geo (accession no. GSE136171).

[1]Present address: Program in Molecular Medicine, University of Massachusetts Medical School, Worcester, MA 01655.

[2]To whom correspondence may be addressed. Email: liangzhou497@ufl.edu.

This article contains supporting information online at https://www.pnas.org/lookup/suppl/doi:10.1073/pnas.1908128116/-/DCSupplemental.

First published November 18, 2019.

mice (*Rag1*$^{-/-}$*Selplg*$^{-/-}$: referred to as RPS), and examined ILC population frequencies among lamina propria lymphocytes (LPLs) in the small and large intestines. We observed a significant decrease of ILC3 (CD3$^-$RORγt$^+$) in the large intestine of RPS mice compared to *Rag1*$^{-/-}$ mice (*SI Appendix*, Fig. S1 *A–D*), but no difference in the small intestine (*SI Appendix*, Fig. S1 *E* and *F*). PSGL-1 was expressed in ILC3s and deleted in RPS mice (*SI Appendix*, Fig. S1*G*). ILC3s are a heterogeneous population of cells, composed of T-bet$^-$ adult lymphoid tissue inducer-like cells, which may or may not express CCR6 or CD4, and T-bet$^+$ cells, which can up-regulate NKp46 (18–20). Both T-bet$^+$ and T-bet$^-$ populations showed decreases in frequency in the large intestine, with a more marked loss in the T-bet$^+$ ILC3 population (*SI Appendix*, Fig. S1 *C* and *D*). T-bet$^+$ ILC (ILC1 and NK cell) frequencies were significantly decreased in RPS compared to control *Rag1*$^{-/-}$ mice (*SI Appendix*, Fig. S1 *A* and *H*). Additionally, we noted an increase in ILC2 frequencies in the large intestine of RPS mice, presumably due to changes in homeostatic balance due to the loss of ILC3s (21) (*SI Appendix*, Fig. S1 *I* and *J*). Together, RPS mice demonstrated significantly reduced ILC3 frequencies in the large intestine with a notable reduction of T-bet$^+$ ILC3s.

A Transmissible Microbiota Population Isolated from *Rag1*$^{-/-}$*Selplg*$^{-/-}$ Mice Suppresses ILC3s in the Colon. Initial experiments compared RPS mice to nonlittermate *Rag1*$^{-/-}$ control mice. Unexpectedly, when we cohoused *Rag1*$^{-/-}$ mice with RPS mice, *Rag1*$^{-/-}$ mice had a reduction of ILC3s (*SI Appendix*, Fig. S1 *K* and *L*). Thus, we performed heterozygous breeding to generate cohoused, littermate mice (Fig. 1*A*). We observed no difference in ILC3 frequency between *Rag1*$^{-/-}$*Selplg*$^{-/-}$ and *Rag1*$^{-/-}$*Selplg*$^{+/-}$ controls. Specifically, *Rag1*$^{-/-}$*Selplg*$^{+/-}$ and RPS littermate mice both showed reduced ILC3 frequencies compared to nonlittermate, noncohoused *Rag1*$^{-/-}$ mice (Fig. 1 *B* and *C*). T-bet$^+$ ILC3s had the most significant decrease in *Rag1*$^{-/-}$*Selplg*$^{+/-}$ mice cohoused with RPS mice (Fig. 1*C*). These data suggested that the ILC3 phenotype observed in RPS littermate mice was transmissible and might be attributed to microbiota that were introduced at the time of generating the double knockout mice, and not directly caused by the *Selplg* gene deficiency. Therefore, to clarify the contribution of the microbiota to the phenotype, we treated the RPS mice with a broad-spectrum mixture of antibiotics (ampicillin, vancomycin, metronidazole, neomycin, and gentamicin). After 12 d of treatment, we observed that ILC3 percentages in RPS mice had increased (Fig. 1 *D* and *E*). Notably, the increase in ILC3s was predominantly in the T-bet$^-$ ILC3 population, but T-bet$^+$ ILC3s

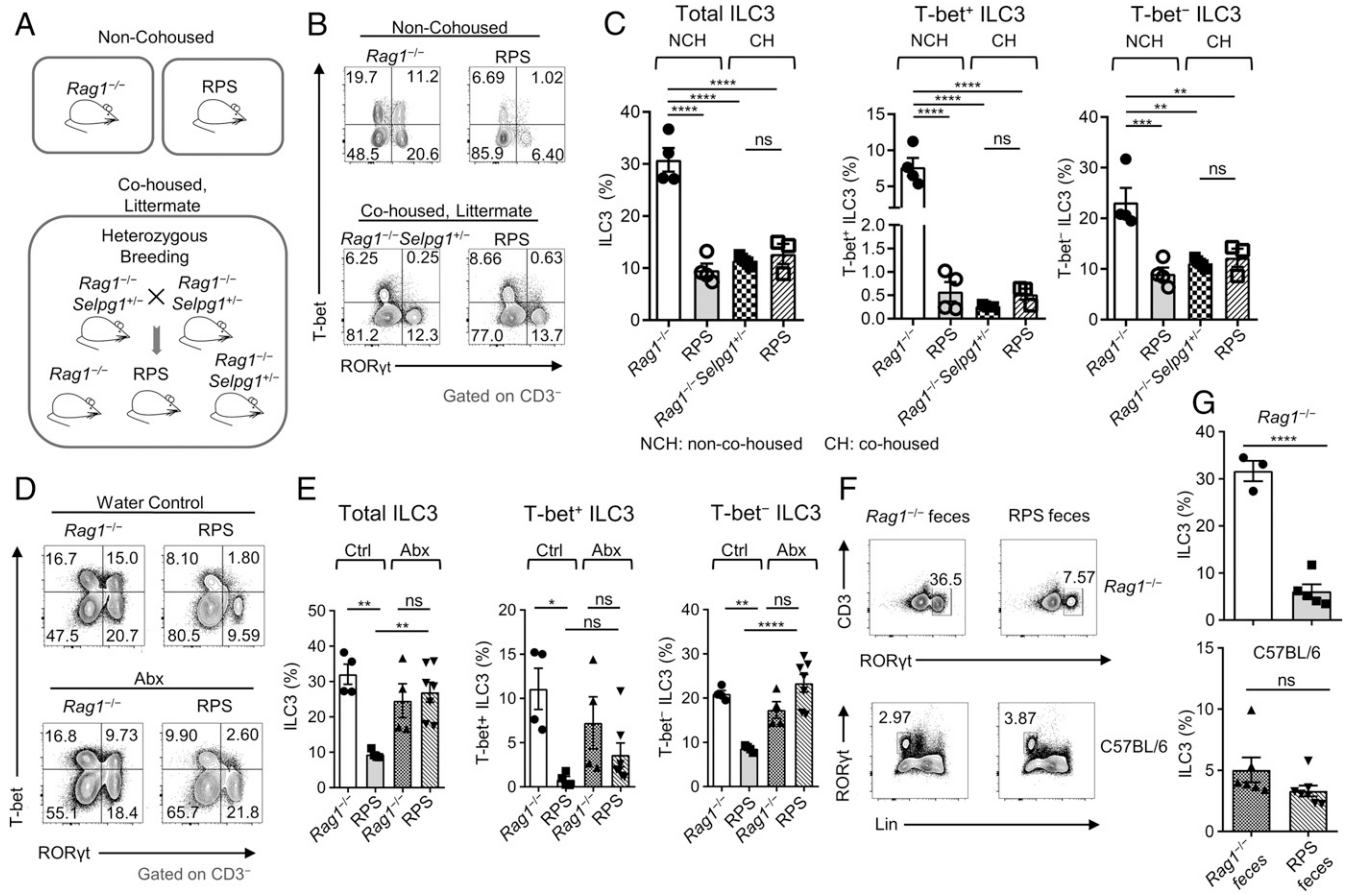

Fig. 1. The microbiota from RPS mice induce a transmissible dysbiois and loss of ILC3s. (*A*) Illustration of mouse housing and breeding scheme. (*B*) FACS plots of RORγt and T-bet staining gated on CD3$^-$ LPLs from the large intestine (LI) from non-cohoused (*Top*) and cohoused (*Bottom*) RPS, *Rag1*$^{-/-}$, or *Rag1*$^{-/-}$*Selpg1*$^{+/-}$ mice. (*C*) Quantification of ILC3 subset frequencies from *Rag1*$^{-/-}$*Selplg*$^{+/-}$ compared to RPS littermate, cohoused (CH) or non-cohoused mice (NCH). Data are pooled from 2 independent experiments ($n = 3$ to 4 per group); one-way ANOVA. (*D*) FACS plots of RORγt and T-bet staining gated on CD3$^-$ LI LPLs from water-treated (Ctrl; *Top*) and antibiotics-treated (Abx; *Bottom*) RPS compared to *Rag1*$^{-/-}$ mice. (*E*) Frequencies of ILC3 subsets in antibiotics-treated mice comparing RPS and *Rag1*$^{-/-}$ mice. Data are pooled from 2 independent experiments ($n = 4$ to 7 per group); one-way ANOVA. (*F*) FACS plots of RORγt and CD3$^-$ staining (*Top*) or Lineage (Lin) and RORγt staining (*Bottom*) gated on LI LPLs. (*G*) Quantification of ILC3 frequencies after indicated feces gavage in the LI of *Rag1*$^{-/-}$ (*Top*; $n = 3$ to 5 per group) and C57BL/6 (*Bottom*; $n = 6$ to 7 per group) mice. Data are pooled from 2 and 3 independent experiments, respectively. Error bars indicate SEM. *$P < 0.05$, **$P < 0.01$, ***$P < 0.001$, ****$P < 0.0001$; ns, not significant.

either did not recover or only partially recovered (Fig. 1 *D* and *E*). Next, we performed a bone marrow transfer experiment to test the contribution of the genotype (*SI Appendix*, Fig. S2*A*). *Rag1*$^{-/-}$ mice were lethally irradiated, and bone marrow from either *Rag1*$^{-/-}$ or RPS mice was transferred intravenously. After 11 wk, we examined ILC3 frequencies. ILC3 frequencies were lower in mice that were irradiated and received a *Rag1*$^{-/-}$ bone marrow transfer compared to nonirradiated *Rag1*$^{-/-}$ mice, presumably due to partial recovery of ILC3s after bone marrow reconstitution. Nonetheless, no difference in ILC3 frequencies was observed in mice that received *Rag1*$^{-/-}$ versus RPS bone marrow (*SI Appendix*, Fig. S2 *B* and *C*), suggesting that the *Selplg* gene deficiency alone could not account for the ILC3 loss. Importantly, gavage of RPS feces into *Rag1*$^{-/-}$ mice reduced ILC3 frequencies compared to *Rag1*$^{-/-}$ feces or PBS controls in the large intestine (Fig. 1 *F* and *G* and *SI Appendix*, Fig. S2 *D*, *F*, *H* and *I*), but not the small intestine (*SI Appendix*, Fig. S2 *E* and *G*), indicating that the ILC3 phenotype was potentially induced by the microbiota in RPS feces. Of note, ILC3s were not reduced when wild-type C57BL/6 mice were gavaged with RPS feces, suggesting that adaptive immunity can prevent the loss of ILC3 after RPS feces gavage (Fig. 1 *F* and *G*).

Feces collected from *Rag1*$^{-/-}$ mice that were previously gavaged with RPS feces, also known as RPS secondary (RPS 2°) feces, could also reduce ILC3 percentages in the colon of *Rag1*$^{-/-}$ mice after gavage, indicating that an actively growing or self-sustaining agent is responsible for the ILC3 reduction in the colon (Fig. 2 *A*–*D*). This was further supported by the result that heat-killed RPS 2° feces could not significantly decrease ILC3s compared to nontreated feces (Fig. 2 *E* and *F*). In contrast, gavage of RPS 2° feces into C57BL/6 mice did not reduce ILC3 frequencies in the large intestine, supporting the finding that adaptive immunity can prevent the loss of ILC3s (*SI Appendix*, Fig. S2*J*). We examined other ILC populations after RPS 2° feces gavage and identified a decrease in ILC1 (Lineage$^-$T-bet$^+$RORγt$^-$EOMES$^-$) frequencies and an increase in ILC2 frequencies (Fig. 2*C*). However, neither ILC1 nor ILC2 cell counts showed significant change after gavage with RPS 2° feces (Fig. 2*H*). There was a significant increase of NK cells (Lineage$^-$T-bet$^+$RORγt$^-$EOMES$^+$) after gavage (Fig. 2 *C* and *D*). Furthermore, similar to the enhanced gut inflammation observed in primary RPS mice (*SI Appendix*, Fig. S3 *A* and *B*), RPS 2° feces gavage resulted in increased inflammation and cell infiltration, which coincided with the loss of ILC3s (*SI Appendix*, Fig. S3 *C* and *D*). Increased neutrophils and eosinophils were observed in the large intestine 12 d after gavage (Fig. 2 *G* and *H*). Together, these data implicated the microbiota as the major

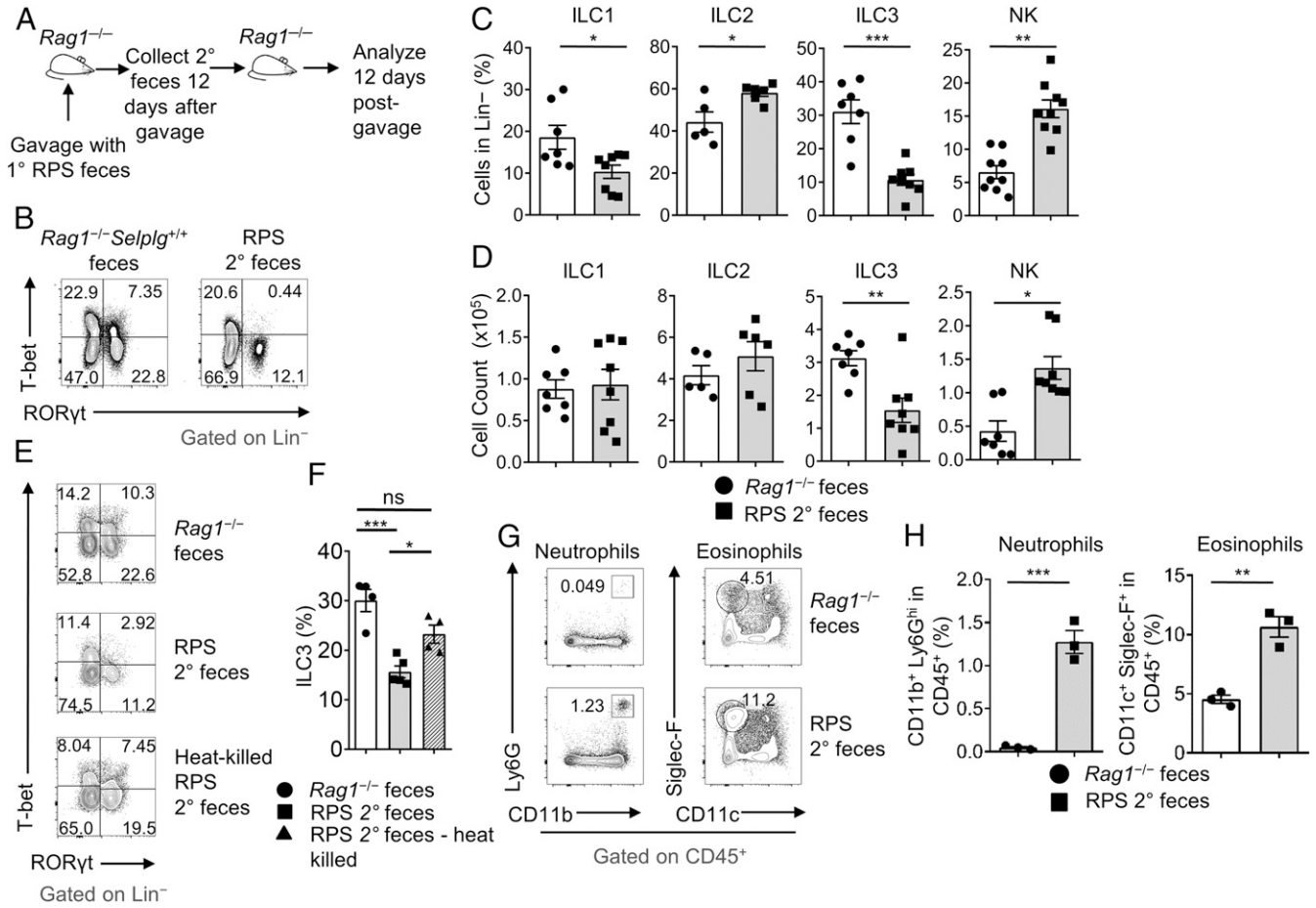

Fig. 2. Serially gavaged RPS feces suppress ILC3 frequencies and are associated with inflammation. (*A*) Illustration of RPS secondary (2°) feces gavage experiment. (*B*) FACS plots of RORγt and T-bet gated on Lin$^-$ LI LPLs. (*C*) Quantification of ILC frequencies and (*D*) counts after gavage with RPS 2° feces or *Rag1*$^{-/-}$ control feces. Data are pooled from 3 independent experiments (n = 5 to 8 per group). (*E*) FACS plots of RORγt and T-bet staining gated on Lin$^-$ LI LPLs. (*F*) Quantification of ILC3 frequencies after gavage with heat-killed or nontreated RPS 2° feces. Data are from 1 experiment (n = 4 to 5 per group); one-way ANOVA. (*G*) FACS plots of (neutrophil; CD11b and Ly6g) and (eosinophil; CD11c and Siglec-F) staining gated on CD45$^+$ LI LPLs. (*H*) Quantification of neutrophil and eosinophil frequencies from *Rag1*$^{-/-}$ mice gavaged with *Rag1*$^{-/-}$ or RPS 2° feces. Data are representative from 1 of 2 independent experiments (n = 3 per group). Error bars indicate SEM. *P < 0.05, **P < 0.01, ***P < 0.001; ns, not significant.

contributing factor to the loss of ILC3s and inflammation observed in RPS mice.

Introduction of RPS Microbiota Changes Gut Transcriptome and Reduces ILC3 Proliferation. Changes initiated by the microbiota in the host colon environment of RPS mice could contribute to the loss of ILC3s. To test this, we examined transcriptional changes in the large intestine of *Rag1*$^{-/-}$ mice 12 d after gavage with RPS 2° feces by RNA sequencing (RNA-seq). Differential gene analysis identified 2,815 significantly changed genes (1,402 down-regulated; 1,413 up-regulated; [q ≤ 0.05; fold change ≥1.5]) in the colon after gavage (Fig. 3*A*). Many of the increased genes were related to inflammation and response to infection, including *Tnf*, *Ifng*, *Il1b*, *Il11*, and *Il6* (Fig. 3*A*). Pathway analysis confirmed that cytokine and chemokine signaling was increased, along with Toll-like and NOD-like receptor pathways (Fig. 3*B* and *SI Appendix*, Fig. S4 *A* and *B*). Detailed examination of chemokines and cytokines revealed that genes *Cxcl1*, *Cxcl2*, *Cxcl3*, *Cxcl9*, and *Cxcl10* related to the chemotaxis of inflammatory cells, such as neutrophils and NK cells, were highly up-regulated, consistent with their increased frequencies, as demonstrated by flow cytometry (Figs. 3*C* and 2 *G* and *H*). Notably, genes related to ILC3 homeostasis were significantly decreased, including *Il7*, *Il15*, and *Kit* (Fig. 3 *A* and *C*). To confirm the RNA-seq results, we examined the transcription of genes in whole colon tissue that are involved in inflammation and ILC homeostasis by quantitative reverse transcription PCR (qRT-PCR). At day 12 after gavage, we observed no significant difference in proinflammatory cytokine transcripts for *Il18 and Il23* (IL-23p19), but a significant increase in *Il12a* (IL-12p35), *Il12b* (IL-12p40), and *Tnf* in the colon (Fig. 3*D*). Previous studies have shown that IL-12 can contribute to ILC3 plasticity, inducing their conversion into ILC1s (22). We observed increased expression of *Il12a* and *Il12b* (Fig. 3*D*), indicating that ILC3 conversion to ILC1 through plasticity was possible in the intestinal environment after gavage.

Changes in homeostatic molecules were confirmed by qRT-PCR, with reductions in both *Il7* and *Il15* transcripts (Fig. 3*E*), both of which have been shown to support ILC3 maintenance in the intestine (23, 24). Similar transcriptional changes of cytokines were observed in the cecum (*SI Appendix*, Fig. S4*C*). We examined the expression of other molecules that may influence the maintenance of ILC3s. Previous studies have shown that increased IL-25 can reduce ILC3 numbers in the intestine (25), but RPS 2° feces-gavaged mice had decreased *Il25* expression (Fig. 3*E*). The aryl hydrocarbon receptor (Ahr) is a key transcription factor involved in the maintenance and function of ILC3s (26–28). We examined transcriptional expression in fluorescence-activated cell sorting (FACS)-purified ILC3s from the large intestine of RPS 2° feces-gavaged mice and did not observe any significant difference in the expression of *Cyp1a1* or *Ahrr* (Fig. 3*F*), indicating no change in Ahr activity. Together, these data indicate that RPS 2° feces gavage can induce a proinflammatory environment with reduced homeostatic molecules.

Reduction of homeostatic cytokines could contribute to reduced proliferation or survival of ILC3s (23, 24, 28). Thus, we performed a kinetic study of the ILC3 compartment after introduction of RPS 2° feces to examine proliferation and survival. Flow cytometry results showed that at day 6 after gavage with RPS 2° feces, ILC3s had a significant reduction in the proliferation marker, Ki-67 (Fig. 3 *G* and *H*). We also observed a reduction in proliferation as early as day 1 and day 3 (*SI Appendix*, Fig. S4 *D–G*). However, no increase in apoptosis, as revealed by Annexin V staining, was observed in ILC3s at any time point (Fig. 3 *G* and *H* and *SI Appendix*, Fig. S4 *D–G*). Additionally, no change in antiapoptotic *Bcl2* expression was observed in sorted ILC3s, suggesting that the loss of ILC3s in the large intestine after RPS 2° feces gavage may be mediated by a reduction in proliferation but not apoptosis (*SI Appendix*, Fig. S4*H*). We examined other potential molecules related to the regulation of ILC3 proliferation at early time points after gavage. Ahr and c-Kit (CD117), an Ahr-regulated growth factor receptor, have been shown to control ILC3 proliferation (18, 26–28). Flow cytometry staining for Ahr and c-Kit found no changes in the expression of either molecule in ILC3s from the large intestine (*SI Appendix*, Fig. S4 *I* and *J*). Together, these results suggest that dysbiosis may lead to the early proliferation changes and reduction of homeostatic promoting factors that are important for sustaining the ILC3 compartment.

***Helicobacter* Species Induce Gut Dysbiosis and Are Associated with the Loss of ILC3s in Immunocompromised Mice.** To identify the microbiota species that may mediate the change in proliferation and loss of ILC3s, we performed 16S rRNA gene sequencing to compare the microbial composition in RPS, *Rag1*$^{-/-}$, and *Rag1*$^{-/-}$ mice cohoused with RPS mice. Sequencing data revealed that compared to *Rag1*$^{-/-}$ mice, RPS mice had perturbed microbiota, characterized by outgrowth of *Lactobacillus*, *Prevotella*, *Allobaculum*, and *Helicobacter* spp. (Fig. 4 *A* and *B*) and decreased bacterial diversity (Shannon Index) (Fig. 4*C*). Notably, this perturbed microbiota was transmissible to cohoused *Rag1*$^{-/-}$ mice (Fig. 4 *A* and *C*).

Prevotella and *Helicobacter* spp. are known pathobionts in immunocompromised mice and may contribute to inflammation (9, 29). To narrow down possible bacterial agents that contributed to the phenotype, we treated mice with a broad-spectrum antibiotics mix (ampicillin, neomycin, vancomycin, metronidazole, and gentamicin) or individually with antibiotics that targeted specific classes of bacteria (e.g., anaerobes, gram-positive, etc.). We observed that loss of ILC3s was mediated by a population of bacteria that were vancomycin and metronidazole resistant but susceptible to gentamicin or a combination of all antibiotics (Fig. 4 *D–F* and *SI Appendix*, Fig. S5*A*). We proceeded to assess the fecal microbial materials from antibiotics-treated mice by 16S rRNA gene sequencing to identify the bacteria that were differentially present among the antibiotics treatment groups. Based on analysis, we identified 4 species that correlated with reduced ILC3s and susceptibility or resistance to the antibiotics combinations: *H. typhlonius*, *Mucispirillum schaedleri*, an unclassified species from the *Coprobacillaceae* family, and an unclassified *Allobaculum* spp. (Fig. 4*H*). Neither *M. schaedleri*, *Allobaculum*, nor *Coprobacillaceae* have been shown to induce inflammation in immunocompetent mice. Rather, they have been associated with outgrowth under inflammatory conditions (30). However, recent work suggests that Nod2- and/or Cybb-deficient mice are susceptible to *Mucispirillum*-induced colitis (31). We examined *M. schaedleri* by qPCR and found its low abundance in mice gavaged with RPS 2° feces (*SI Appendix*, Fig. S5*B*). *Helicobacter* spp. have been known to initiate inflammation in immune-deficient mice (10, 17). We found in our gavage experiments that higher *H. typhlonius* shed in the feces of mice strongly correlated with lower total large intestinal (Pearson $r = -0.84$, P value <0.0001), T-bet^{+}, and T-bet^{-} ILC3 frequencies (Fig. 4*I*); hence, the expansion of *H. typhlonius* in RPS mice warranted further investigation.

***H. typhlonius* and *H. apodemus* Promote the Loss of Colonic ILC3s.** *H. typhlonius* induces murine colitis within an immunocompromised background, such as *Il10*$^{-/-}$, *Prkdc*^{scid}, and *Tbx21*$^{-/-}$*Rag2*$^{-/-}$ mice (17, 32, 33). Thus, we aimed to isolate the *Helicobacter* spp. that may be responsible for the observed phenotypes (i.e., reduction of ILC3s) from RPS 2° feces. While *H. apodemus* (Massachusetts Institute of Technology, MIT 18-1095S) was present in both *Rag1*$^{-/-}$ and RPS 2° feces, *H. typhlonius* (MIT 18-1095F) was identified only in RPS 2° feces (*SI Appendix*, Fig. S6*A*). To elucidate the contribution of these specific species to the ILC phenotype observed, we gavaged *Rag1*$^{-/-}$ mice with either

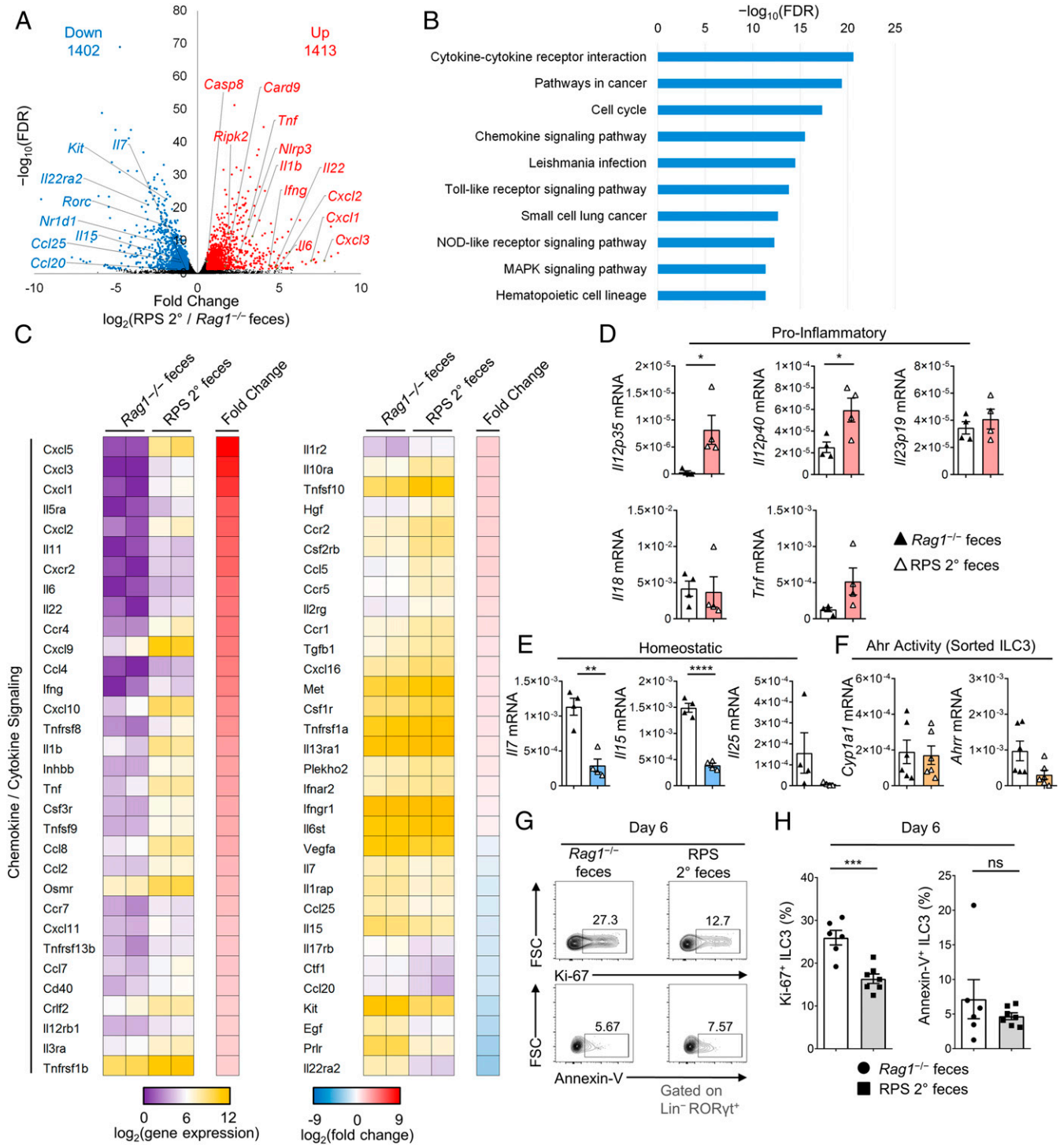

Fig. 3. The microbiota from RPS mice induces colonic transcriptional changes that result in and reduce ILC3 proliferation. (*A*) Volcano plot of significantly up-regulated (up) and down-regulated (down) genes in the LI of *Rag1*$^{-/-}$ mice gavaged with RPS 2° or *Rag1*$^{-/-}$ feces. (*B*) The top pathways identified by pathway analysis of differentially regulated genes using the Kyoto Encyclopedia of Genes and Genomes database. (*C*) Heatmap of cytokine or chemokine gene expression and fold change. Data are representative from 1 experiment with 2 biological replicates per group. (*D*) Gene expression relative to *Actin* as measured by qRT-PCR for indicated proinflammatory and (*E*) ILC homeostatic genes expressed in the proximal colon of mice gavaged with RPS 2° or *Rag1*$^{-/-}$ feces. (*F*) Gene expression relative to *Actin* as measured by qRT-PCR for Ahr target genes in FACS-purified ILC3s from the LI of mice gavaged with RPS 2° or *Rag1*$^{-/-}$ feces. Data are representative from 1 of 2 independent experiments ($n = 4$ to 6 per group). (*G*) FACS plots of Ki-67 (*Top*) and Annexin V (*Bottom*) staining gated on Lin^{-} RORgt^{+} LI LPLs. (*H*) Quantification of Ki-67^{+} (*Left*) and Annexin V^{+} (*Right*) ILC3 frequencies in LI LPLs at day 6 after gavage with RPS 2° or *Rag1*$^{-/-}$ feces. Data are pooled from 2 independent experiments ($n = 6$ to 7 per group). Error bars indicate SEM. *$P < 0.05$, **$P < 0.01$, ***$P < 0.001$, ****$P < 0.0001$; ns, not significant.

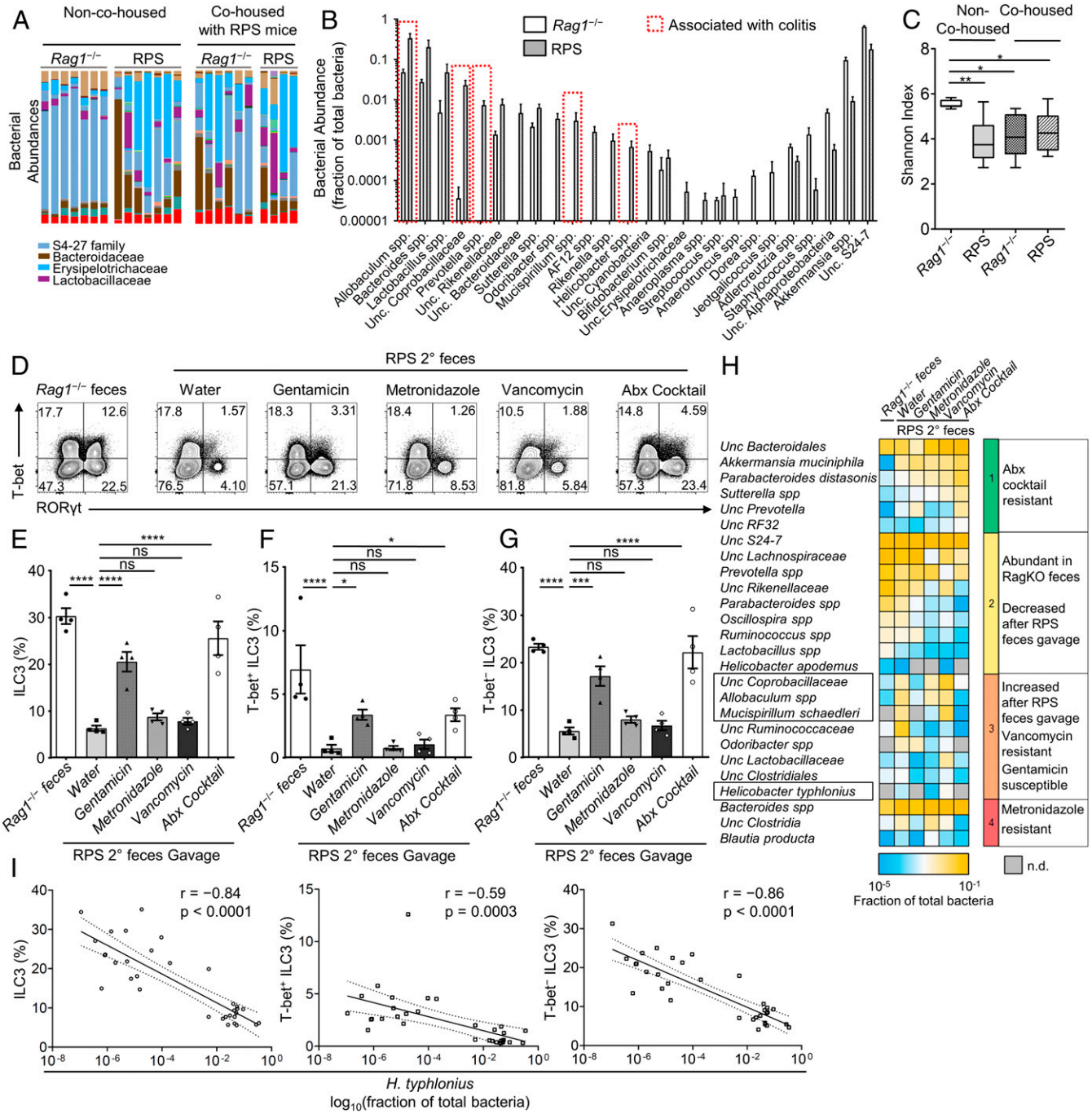

Fig. 4. *H. typhlonius* is associated with gut dysbiosis and loss of ILC3s. (*A*) Bacterial (family) abundances by 16S rRNA gene sequencing in non-cohoused or cohoused *Rag1*$^{-/-}$ and RPS mice. (*B*) Quantification of bacterial abundance as a fraction of total bacteria for significantly changed ($P \leq 0.05$, Mann–Whitney test) species; unclassified (Unc.). (*C*) Shannon Index measuring bacterial diversity of non-cohoused and cohoused *Rag1*$^{-/-}$ and RPS mice. Data are representative from 1 experiment with 4 to 7 biological replicates per group; one-way ANOVA. (*D*) FACS plots of RORγt and T-bet staining gated on LI LPLs. (*E*) Quantification of total, (*F*) T-bet^{+} and (*G*) T-bet^{-} ILC3 frequencies in LI LPLs from RPS 2° feces-gavaged *Rag1*$^{-/-}$ mice after antibiotics treatment. Data are pooled from 2 independent experiments ($n = 4$ per group); one-way ANOVA compared to water control mean. (*H*) Heatmap indicating the abundance of bacteria as measured by 16S rRNA gene sequencing after selective antibiotics treatment or untreated controls (n.d., not detected). Data are representative from 1 experiment with 2 biological replicates per group. (*I*) Scatterplots indicating *H. typhlonius* abundance compared to total (*Left*), T-bet^{+} (*Center*), or T-bet^{-} (*Right*) ILC3 frequencies. Regression lines (solid) and 95% confidence intervals (dashed) are plotted. Pearson correlation (*r*) and *P* value are indicated. Data are pooled from 5 experiments ($n = 33$). Error bars indicate SEM. *$P < 0.05$, **$P < 0.01$, ***$P < 0.001$, ****$P < 0.0001$; ns, not significant.

H. apodemus, *H. typhlonius*, or a mixture of the 2 bacteria to examine ILC populations 12 d later (*SI Appendix*, Fig. S6*B*). As a control, we used *Helicobacter rodentium*, another *Helicobacter* spp. that colonizes mice but was absent in our colony of *Rag1*$^{-/-}$ mice (*SI Appendix*, Fig. S6*B*). Compared to *H. rodentium*, gavage with *H. apodemus* and/or *H. typhlonius* (single or combined transfaunation) reduced large intestinal ILC3s (Fig. 5 *A* and *B*), particularly T-bet^{+}RORγt^{+} ILC3 (Fig. 5 *C* and *D* and *SI Appendix*, Fig. S6*C*), and increased NK cell frequencies and counts (Fig. 5 *E* and *F* and *SI Appendix*, Fig. S6*D*), consistent with the phenotype observed

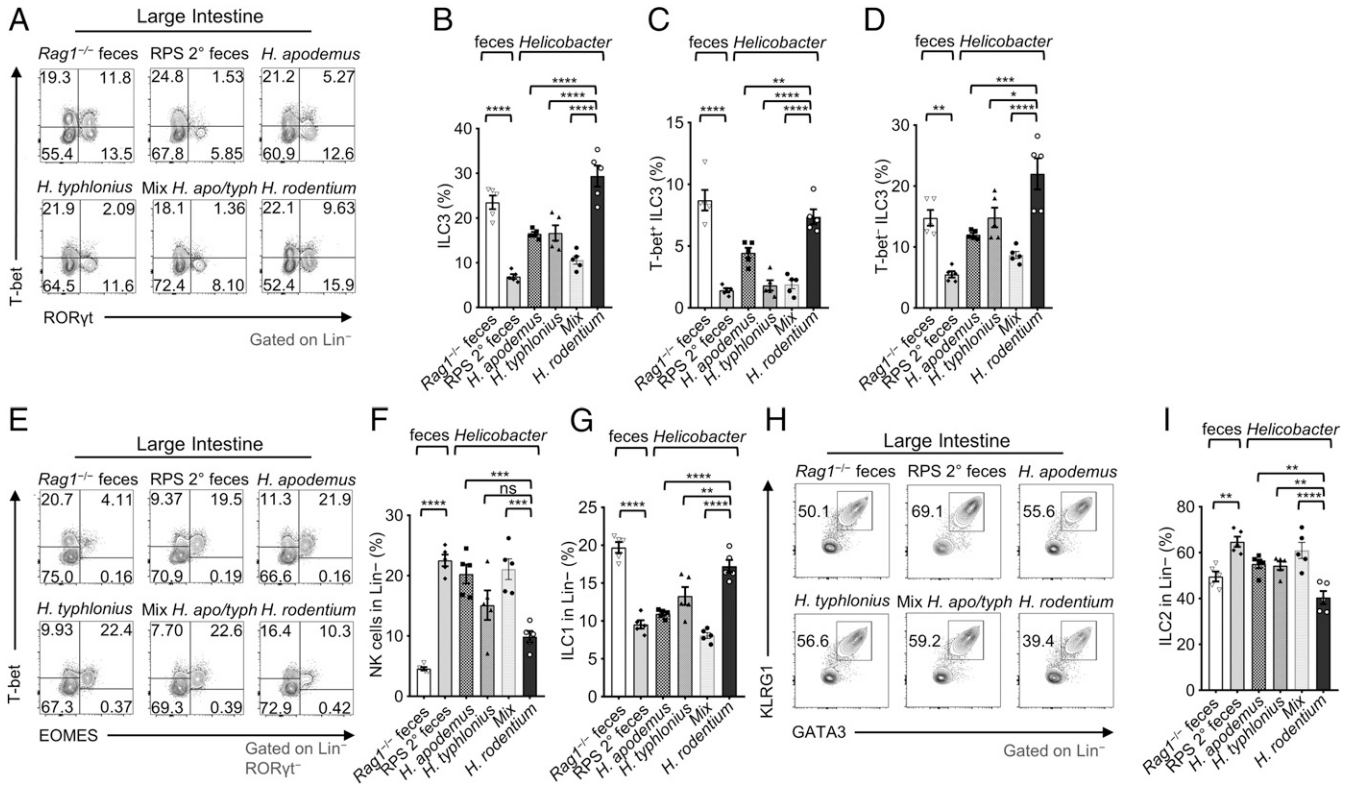

Fig. 5. *H. typhlonius* and *H. apodemus* promote the loss of ILC3s in the large intestine. (*A*) FACS plots of RORγt and T-bet staining gated on Lineage$^-$ LI LPLs. (*B*) Quantification of ILC3, (*C*) T-bet$^+$, and (*D*) T-bet$^-$ ILC3 frequencies in LI LPLs of mice gavaged with feces or *Helicobacter* spp. (*E*) FACS plots of EOMES and T-bet staining gated on Lineage$^-$ RORγt$^-$ LI LPLs. (*F*) Quantification of ILC1 (RORγt$^-$T-bet$^+$EOMES$^-$) and (*G*) NK cells (RORγt$^-$T-bet$^+$EOMES$^+$) in LI LPLs of mice gavaged with feces or *Helicobacter* spp. (*H*) FACS plots of GATA3 and KLRG1 staining gated on Lineage$^-$ LI LPLs. (*I*) Quantification of ILC2 frequencies in LI LPLs of mice gavaged with feces or *Helicobacter* spp. Data are pooled from 3 independent experiments ($n = 5$); one-way ANOVA. Error bars indicate SEM. $^*P < 0.05$, $^{**}P < 0.01$, $^{***}P < 0.001$, $^{****}P < 0.0001$; ns, not significant.

after gavage with RPS 2° feces. In addition, gavage with *H. typhlonius* reduced the frequencies of Ki-67$^+$ T-bet$^-$ ILC3s, but not Ki-67$^+$ T-bet$^+$ ILC3s, in the large intestine, similar to RPS 2° feces (*SI Appendix*, Fig. S5*C*). This observation supports the reduction of T-bet$^-$ ILC3s, but cannot account for the loss of T-bet$^+$ ILC3s. Of note, endogenous *H. apodemus* (MIT 18-1095S) present in *Rag1*$^{-/-}$ mice did not cause a reduction of ILC3s but transfaunation of pure *H. apodemus* bacteria with large quantities led to reduced ILC3s (Fig. 5 *A* and *B*). When we examined other ILC populations, we found that large intestinal ILC1 frequencies and cell counts were reduced in mice after gavaging with *H. apodemus* and/or *H. typhlonius* (Fig. 5 *E* and *G* and *SI Appendix*, Fig. S6*D*). ILC2 frequencies slightly increased, but there was a decrease in cell number (Fig. 5 *H* and *I* and *SI Appendix*, Fig. S6*D*). Together, these data suggest the differential role of *Helicobacter* spp. in regulating different subsets of ILCs.

***Helicobacter* spp. Activate ILC Function and Induce Inflammation.** We further determined the effect of *Helicobacter* spp. on the function of ILCs. We observed increased IL-22$^+$, GM-CSF$^+$, or IL-17A$^+$ ILC3 frequencies (Fig. 6 *A*–*C*), and their absolute numbers were decreased or unchanged in RPS feces-gavaged mice and in mice transfaunated with *Helicobacter* spp. except for *H. rodentium* (*SI Appendix*, Fig. S6 *E*–*G*). These data suggest that *Helicobacter* spp. induce activation of ILC3s, consistent with previous reports (14–17); however, *H. typhlonius* and *H. apodemus* but not *H. rodentium* reduce ILC3 numbers. Similar to the RPS 2° feces gavage, transfaunation of mice with either *H. typhlonius* or *H. apodemus* induced a strong IFN-γ response, notably expressed by ILC1s and infiltrating NK cells but not by ILC3s (Fig. 6 *D*–*F*). We also observed an increase of a lineage$^+$ (CD3, CD19, and Ly6g) IFN-γ$^+$ population of cells in mice gavaged with RPS 2° feces, *H. typhlonius*, *H. apodemus*, or mixed treatments that was absent in *H. rodentium*-gavaged mice (Fig. 6 *G*–*I*). In *Rag1*$^{-/-}$ mice, this lineage$^+$ population is likely infiltrating Ly6g$^+$ neutrophils. These data indicate that *H. apodemus* and *H. typhlonius*, may cooperatively contribute to the loss of T-bet$^+$ ILCs and the induced inflammation. Indeed, the mixed 50:50 *Helicobacter* transfaunation treatment most closely resembled results obtained in mice gavaged with RPS 2° feces (Fig. 5*B*). However, this does not exclude the possibility that other bacterial species endogenous to the resident mouse colony or enriched in the RPS feces, including *Prevotella* and *Mucispirillum* spp., potentially contribute to the described phenotypes (Fig. 4 *B* and *H*). Together, these data demonstrated that *Helicobacter* spp. activate ILC function by enhancing their cytokine production.

We speculated that the loss of ILC3s might result in altered immunity of mice transfaunated with *H. typhlonius* or *H. apodemus*. To this end, we determined the action of *Helicobacter* in 2 models of colitis, dextran sodium sulfate (DSS)-induced colitis and *Citrobacter rodentium* infection, both of which depend on ILC3s for protective immunity (25, 34, 35). We induced DSS colitis after *Helicobacter* spp. gavage and found that *Helicobacter*-gavaged mice had increased weight loss compared to *Rag1*$^{-/-}$ feces-gavaged control mice (*SI Appendix*, Fig. S7 *A* and *B*). Intriguingly, the *H. rodentium*-gavaged control mice, which did not show a reduction of ILC3s after gavage (Fig. 5*A*), had increased weight loss, consistent with more inflammatory cytokine production (e.g., IFN-γ) by ILC3s (Fig. 6 *A*–*C* and *SI Appendix*, Fig. S6 *E*–*G*) that can influence the DSS colitis phenotype

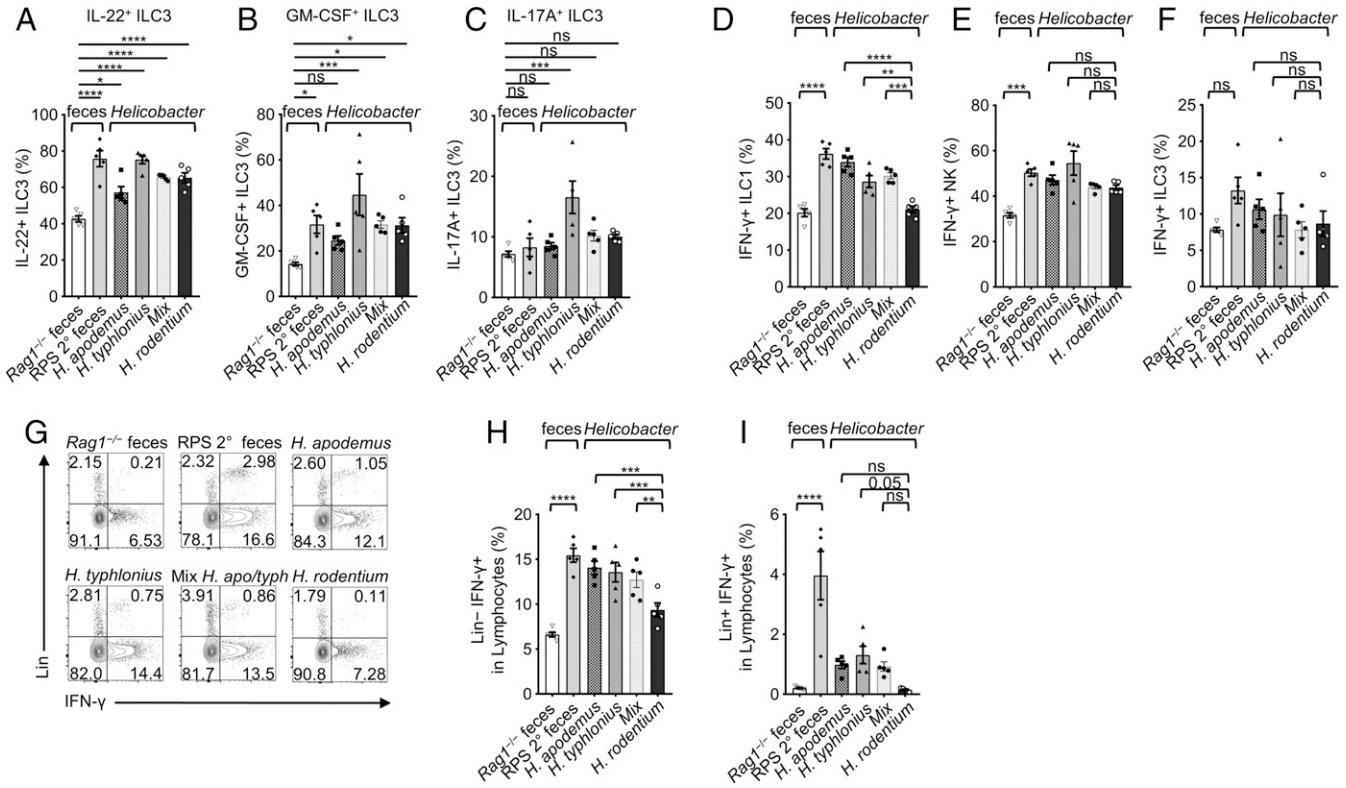

Fig. 6. *H. typhlonius* and *H. apodemus* enhance ILC function. (*A*) Quantification of IL-22$^+$, (*B*) GM-CSF$^+$, and (*C*) IL-17A$^+$ ILC3s frequencies in LI LPLs of mice gavaged with feces or *Helicobacter* spp.; one-way ANOVA compared to the mean of *Rag1*$^{-/-}$ control. (*D*) Quantification of IFN-γ$^+$ ILC1, (*E*) NK, and (*F*) ILC3 frequencies after gavage with feces or *Helicobacter* spp. (*G*) FACS plots of IFN-γ and Lineage (CD3, CD19, and Ly6g) staining gated on LI LPLs. (*H*) Quantification of Lin$^+$ and (*I*) Lin$^-$ IFN-γ$^+$ LI LPLs from mice gavaged with feces or *Helicobacter* spp. Data are pooled from 3 independent experiments ($n = 5$); one-way ANOVA. Error bars indicate SEM. *$P < 0.05$, **$P < 0.01$, ***$P < 0.001$, ****$P < 0.0001$; ns, not significant.

(e.g., wasting disease) (*SI Appendix*, Fig. S7*B*). Since DSS treatment caused ILC3 reduction in *Rag1*$^{-/-}$ mice compared to *Rag1*$^{-/-}$ mice at the steady state (*SI Appendix*, Figs. S7*C* and S1 *A* and *B*), the role of *Helicobacter* spp. in regulating ILC3-mediated protection was unclear in the aforementioned model.

Consistent with DSS-induced wasting disease, during *C. rodentium* infection, *Helicobacter* spp. gavage led to more body weight loss (*SI Appendix*, Fig. S7 *D* and *E*). Moreover, *Helicobacter*-gavaged mice had more dissemination of bacteria to the spleen compared to *Rag1*$^{-/-}$ mouse feces-gavaged control mice (*SI Appendix*, Fig. S7*F*). Together, these data suggest that *Helicobacter* spp. may induce prolonged colonic inflammation and tissue damage that lead to dissemination and wasting disease.

Discussion

We started our investigation examining the role of PSGL-1 in ILC biology, but discovered an important interaction between the microbiota and host immune cells. We favored the possibility that RPS mice acquired, by chance, pathobiont *Helicobacter* species in our mouse facility. These *Helicobacter* function as key contributors to the reduction of ILC3s in the large intestines of mice that lack adaptive immunity. However, we could not rule out the possibility that PSGL-1 deficiency helped initiate the fortuitous outgrowth of the *Helicobacter* spp. in RPS mice. Further study is needed to determine if loss of PSGL-1 is an initiating factor or dispensable for the observed phenotype. Nevertheless, our data show that in *Helicobacter*-gavaged *Rag1*$^{-/-}$ mice, inflammation and pathology, as noted by increased cell infiltration and cytokine expression, is negatively correlated with the frequency of ILC3s. It remains to be determined if the loss of ILC3s is responsible for gut inflammation or vice versa.

Individual ILC3 subset (T-bet$^+$ vs. T-bet$^-$) responses to RPS feces or *Helicobacter* spp. gavage differed in our experiments. Our data showed that treatment of RPS feces-transferred *Rag1*$^{-/-}$ mice with antibiotics results in more significant restoration of the T-bet$^-$ ILC3 population. However, *Helicobacter* spp. treatment suppressed the T-bet$^+$ but not T-bet$^-$ ILC3s. The 16S rRNA gene sequencing shows in addition to *Helicobacter* spp., the expansion/enrichment of *Prevotella*, *Mucispirillum*, and other colitis-associated bacteria in the RPS feces. The differences in the ILC3 subset responses to RPS feces versus *Helicobacter* spp. gavage may be influenced by these additional bacteria. In addition, changes in proliferation observed after RPS feces or *Helicobacter* spp. gavage distinctly affected T-bet$^-$, but not T-bet$^+$, ILC3s.

There are 2 major subsets of ILC3s. T-bet$^+$ ILC3s are CCR6$^-$ and can up-regulate NKp46. On the other hand, T-bet$^-$ ILC3s may or may not express CCR6 or CD4 (18–20). Previous work has shown that T-bet$^+$CCR6$^-$ ILC3 numbers are influenced by signals from the microbiota, as germ-free mice had lower numbers compared to mice raised in specific pathogen-free (SPF) conditions (18–20). Our data showed that the numbers of T-bet$^+$ CCR6$^-$ ILC3s were reduced by the introduction of *Helicobacter* spp. Precise mechanisms remain to be determined and may involve either a direct impact on those specific ILC3 subsets or an indirect mechanism of dysbiosis, consistent with the reduced microbial diversity upon RPS fecal treatment. In addition, it has been shown that T-bet$^-$CCR6$^-$ ILC3s can up-regulate T-bet, some of which can lose RORγt (18, 23). Thus, plasticity of ILC3s may also account for the reduction of T-bet$^+$ ILC3s. Together, these data indicate multiple mechanisms may affect the maintenance of T-bet$^-$ versus T-bet$^+$ ILC3s in mice gavaged with RPS feces or *Helicobacter* spp.

Novel nongastric *Helicobacter* spp. are increasingly identified in cases of diarrhea and bacteremia in humans and animals (10, 36, 37). *Helicobacter hepaticus* infection in immunocompromised mice has been widely used as a model of inflammatory bowel disease, and chronic inflammation induced by *H. hepaticus* infection in *Rag2*$^{-/-}$ mice promotes tumor formation in the colon (9, 14, 38). Similarly, we identified increased proinflammatory cytokines after *H. apodemus* or *H. typhlonius* gavage in *Rag1*$^{-/-}$ mice. Powell (17) showed that *H. typhlonius* promoted gastrointestinal pathology in *Tbx21*$^{-/-}$*Rag2*$^{-/-}$ ulcerative colitis (TRUC) mice. Additionally, they found that IL-17A–producing ILCs contributed to the colitis, implicating ILC3s (17). Accordingly, treatment with agents that deplete ILCs (e.g., anti-CD90 and anti–IL-7Ra antibodies) reduced the pathology of *Helicobacter*-induced colitis (14, 17). Consistently, our data showed that transfaunation of *Helicobacter* spp. can increase production of IL-17A, IFN-γ, and GM-CSF by ILCs in *Rag1*$^{-/-}$ mice. Thus, these data indicate that ILC3s may play a pathogenic role by producing proinflammatory cytokines in immune-compromised mice lacking the adaptive immune system (14–16).

In the presence of adaptive immunity, ILC3 induction/activation by *Helicobacter* spp. plays a protective role by limiting effector T cell responses toward *Helicobacter* spp. Indeed, a recent study found that ILC3s negatively regulate the adaptive immune response to *H. typhlonius* (39). Antigen presentation by ILC3s suppresses the effector T cell response to *H. typhlonius*, suggesting that ILC3s, along with regulatory T cells, may be responsible for limiting effector T cell-mediated pathology in response to *Helicobacter* spp. in the colon. *H. typhlonius* and *H. apodemus* are both potent inducers of antigen-specific effector and regulatory T cell responses (12). The addition of IL-10 receptor blocking antibodies in a model of DSS-induced colitis results in the expansion of *H. typhlonius* and *H. apodemus* in the population of mucosa-associated bacteria. This is consistent with previous reports indicating that IL-10–deficient mice are particularly susceptible to colonization by enteric *Helicobacter* spp., and that regulatory T cells suppress *Helicobacter*-induced pathology, dependent on IL-10 (13, 33). In our study, C57BL/6 wild-type mice gavaged with *Helicobacter* do not lose ILC3s, unlike *Rag1*-deficient mice, suggesting that the adaptive immunity could sustain ILC3s in the presence of *Helicobacter* spp. These data suggest a balance between the induction of innate immunity and effector T cells by *Helicobacter* spp., and the induction of regulatory responses (e.g., regulatory T cells).

Factors from *H. apodemus or H. typhlonius* may work directly or indirectly on immune cells in the colon. Further study is required to identify and test specific factors from these species. Genomic sequencing of *H. typhlonius* and *H. apodemus* indicate that these bacteria contain a number of virulence factors whose contribution to the ILC3 phenotype would need to be tested through knockout mutations (40, 41). Nonetheless, in this study we discovered that *H. apodemus* and *H. typhlonius* introduction into immunocompromised mice are suppressive of ILC3s, and can serve as a model for future investigations of the host–microbe interactions that maintain ILC3s in the gut.

Materials and Methods

Mice. All of the mice in this study were maintained in SPF facilities at Northwestern University or later at the University of Florida. Mice were of both sexes, littermates, and 6 to 10 wk old unless otherwise indicated. C57BL/6 and *Rag1*$^{-/-}$ were purchased from The Jackson Laboratory. *Rag1*$^{-/-}$ mice were crossed with *Selplg*$^{-/-}$ mice to generate *Rag1*$^{-/-}$*Selplg*$^{-/-}$ mice. The institutional animal care and use committees of Northwestern University and the University of Florida approved all studies with mice.

Bacterial Cultures, Fecal Collection, and Administration. *H. apodemus* (MIT 18-1095S), *H. typhlonius* (MIT 18-1095F), which were isolated from the feces of RPS mice in the same colony, and *H. rodentium* (ATCC700285) were grown under microaerobic conditions in a vented jar containing N_2, H_2, and CO_2 (80:10:10) at 37 °C on 5% sheep blood agar plates for 2 to 3 d. Bacteria were collected and resuspended in *Brucella* broth with 20% glycerol, and the bacteria concentration was adjusted to 1 OD_{600}/mL. Mice were orally gavaged with 200 μL inoculum every other day, a total of 3 times. Freshly collected feces from *Rag1*$^{-/-}$, RPS, or mice previously gavaged with RPS feces were homogenized in 20% glycerol in sterile PBS and stored as a slurry at −80 °C. Fecal slurries were pooled, centrifuged, and washed with sterile PBS before resuspension in sterile PBS for gavage (200 μL per mouse, once).

Antibiotics Treatments. Mice were treated for 12 d with a broad-spectrum mixture of antibiotics (ampicillin [1 g/L], vancomycin [0.5 g/L], metronidazole [1 g/L], neomycin [1 g/L], and gentamicin [1 g/L]) or with individual antibiotics at the indicated concentrations in their drinking water.

Isolation of Lymphocytes from Intestinal Lamina Propria and Flow Cytometry. Isolation of intestinal lamina propria cells and flow cytometry were done as previously described (28). CD16/32 antibody (eBioscience) was used to block the nonspecific binding to Fc receptors before surface staining. Lymphocytes isolated from intestinal lamina propria were stained with antibodies against the following markers: GATA3 (APC, PE-Cy7), RORγt (Brilliant Violet 421, PE), T-bet (PE-Cy7), Eomes (PerCP-eFluor 710), Ahr (APC), CD117 (PE), KLRG1 (PerCP-eFluor 710), CD3 (FITC), CD4 (Alexa Fluor 488, Brilliant Violet 510), NKp46 (PerCP-eFluor 710, Brilliant Violet 510), GM-CSF (Alexa Fluor 488), IFN-γ (APC), IL-22 (APC), IL-17A (PerCP-eFluor 710), CD45.2 (APC, PerCP-Cy5.5), CD11b (PerCP/Cy5.5), CD11c (PE-Cy7), and Siglec-F (Brilliant Violet 421). For staining of ILC1 and NK cells, Lineage marker mix (Lin) contained APC-Cy7 or APC-eFluor 780-CD3, CD19, and Ly6G. For staining of ILC2 and ILC3 cells, Lin referred to a combination of lineage markers: APC-Cy7 or APC-eFluor 780-CD3, CD5, CD19, B220, CD11b, CD11c, Ter119, and Ly6G. For nuclear transcription factor staining, cells were fixed and permeabilized with Foxp3 staining buffer kit (eBioscience). For cytokine staining, cells were stimulated with 50 ng/mL phorbol 12-myristate 13-acetate and 500 ng/mL ionomycin for 4 h and Brefeldin A (2 μg/mL) was added 2 h before cells were harvested. The live and dead cells were discriminated by Live/Dead violet viability kit (Invitrogen) or Zombie Aqua Fixable Viability Kit (Biolegend).

qRT-PCR. RNA from proximal colon tissue (30 mg) from *Rag1*$^{-/-}$ mice gavaged with *Rag1*$^{-/-}$ feces or RPS 2° feces was isolated with TRIzol reagent (Invitrogen). cDNA was synthesized using GoScript Reverse Transcription kit (Promega). Fecal DNA was extracted by Quick-DNA Fecal/Soil Microbe kit (Zymogen Research) or E.Z.N.A. Stool DNA kit (Omega Bio-tek). RT-PCR was performed using SYBR Green (Biorad) with the primers in *SI Appendix*, Table S1. Measurements were made in duplicate wells, and results were normalized to those obtained with *Actin* for mouse genes and universal 16S rRNA gene primers for bacteria.

RNA-Seq and Analysis. Whole proximal colon tissue (30 mg) from *Rag1*$^{-/-}$ mice gavaged with *Rag1*$^{-/-}$ feces or RPS 2° feces (2 biological replicates for each group) was homogenized in TRIzol reagent (Invitrogen). RNA was subsequently extracted and total RNA was treated with a poly-A enrichment kit and RNA-seq libraries were generated. Barcoded samples were pooled and sequenced over 1 lane on an Illumina HiSeq 2500 instrument (University of Chicago Genomics Core) to produce 50-bp single-end reads. Demultiplexed raw data files from the sequencing core were analyzed for quality control using FastQC (Babraham Bioinformatics). Reads were mapped (STAR aligner) to the mm10 assembly of the *Mus musculus* genome (National Center for Biotechnology Information) and filtered for uniquely mapped reads. Genome visualization tracks (bedgraph files) were uploaded to the University of California Santa Cruz Genome Browser for visual comparison of expression levels. Quantitated relative mRNA expression levels (normalized read counts) were calculated based on exon regions using STAR and the mm10 reference genome annotations. Significantly changed genes were identified by DESeq2. Genes found to be significantly changed (q value ≤0.05; fold change ≥1.5) were used for pathway analysis with GSEA software and the Molecular Signature Database (MSigDB).

16S rRNA Gene Sequencing and Analysis. For microbiome analyses, fecal DNA was isolated and amplified with Illumina MiSeq compatible primers, targeting the 16S rRNA gene V4–V5 region. Amplicons were purified by QIAquick Gel Extraction kit (Qiagene, Madison, WI) and quantified by Qubit 2.0 Fluorometer (Invitrogen, Grand Island, NY) and Kapa SYBR fast qPCR kit (Kapa Biosystems, Inc., Woburn, MA). Equal amounts of amplicons were pooled with 10% of Phix control to generate the DNA library. Sequencing was performed on the Illumina MiSeq (Illumina, Inc., San Diego, CA). Sequence analyses were performed using QIIME v.1.9.0. After checking the quality of the sequenced reads, 8-nucleotide (nt) barcodes were extracted

from both forward and reverse reads to generate a barcode library. Forward and reverse reads were then joined, and sequence libraries were split based on their corresponding barcodes. We used an open reference operational taxonomic unit (OTU) picking strategy to select OTUs (with 97% identity threshold). Taxonomy was assigned based on the Greengenes reference database. A taxonomic table for each taxonomic level was generated based on the OTU table and bar charts were generated. Differentially significant features at each level were identified by Mann–Whitney *U* (pairwise comparisons) or Kruskall–Wallis test ($P < 0.05$).

Bone Marrow Transfer. Bone marrow (4×10^6 cells in total) from *Rag1*$^{-/-}$ or RPS mice was i.v. injected into *Rag1*$^{-/-}$ mice irradiated at 550 rads twice with 5-h intervals. Recipient mice were treated with antibiotics (sulfamethoxazole and trimethoprim suspension, Hi-Tech Pharmacal) for 2 wk after injection and analyzed 11 wk after transfer.

***C. rodentium* Infection and Colony-Forming Units.** *C. rodentium* (DBS100, ATCC51459) was cultured overnight in LB medium and the cell density was determined by OD_{600} measurement. A total of 10^{10} colony-forming units (CFUs) of bacteria in 200 μL PBS was gavaged orally into each mouse. Body weight was monitored at indicated time points. Fecal contents were plated on MacConkey plates after serial dilution, and the CFUs of *C. rodentium* were counted and normalized to fecal weight after incubation at 37 °C for 24 h.

DSS-Induced Colitis. DSS colitis was induced in mice by providing 2.5% (wt/vol) DSS (molecular mass = 36 to 50 kDa, MP Biomedicals) in drinking water for 6 d. Mice were monitored daily for body weight loss, stool consistency, and blood in the stool.

Statistical Methods. Unless otherwise noted, statistical analysis was performed with the unpaired 2-tailed Student's *t* test on individual biological samples with GraphPad Prism 8.0. One-way ANOVA analyses are corrected for multiple comparisons. $*P < 0.05$, $**P < 0.01$, $***P < 0.001$, $****P < 0.0001$; ns, not significant.

Data Availability. All data discussed in the paper have been made available to readers.

ACKNOWLEDGMENTS. We thank the entire L.Z. laboratory for help and suggestions. We thank Jacob Weiderman for assistance with the preparation and performance of 16S rRNA gene sequencing. We thank the Genomics Facility (The University of Chicago) for sequencing services and assistance. The work was supported by the NIH (AI132391 and DK105562 to L.Z.). L.Z. is a Pew Scholar in Biomedical Sciences, supported by the Pew Charitable Trusts, and an Investigator in the Pathogenesis of Infectious Disease, supported by the Burroughs Wellcome Fund. J.W.B. is partially supported by a supplement to DK105562. This work was made possible in part by NIH Instrumentation Grant 1S10 OD021676-01.

1. J. W. Bostick, L. Zhou, Innate lymphoid cells in intestinal immunity and inflammation. *Cell. Mol. Life Sci.* **73**, 237–252 (2016).
2. M. Ebbo, A. Crinier, F. Vély, E. Vivier, Innate lymphoid cells: Major players in inflammatory diseases. *Nat. Rev. Immunol.* **17**, 665–678 (2017).
3. G. Gasteiger, X. Fan, S. Dikiy, S. Y. Lee, A. Y. Rudensky, Tissue residency of innate lymphoid cells in lymphoid and nonlymphoid organs. *Science* **350**, 981–985 (2015).
4. Y. Huang *et al*., IL-25-responsive, lineage-negative KLRG1(hi) cells are multipotential 'inflammatory' type 2 innate lymphoid cells. *Nat. Immunol.* **16**, 161–169 (2015).
5. M. B. M. Teunissen *et al*., Composition of innate lymphoid cell subsets in the human skin: Enrichment of NCR(+) ILC3 in lesional skin and blood of psoriasis patients. *J. Invest. Dermatol.* **134**, 2351–2360 (2014).
6. F. Villanova *et al*., Characterization of innate lymphoid cells in human skin and blood demonstrates increase of NKp44+ ILC3 in psoriasis. *J. Invest. Dermatol.* **134**, 984–991 (2014).
7. W. Haddad *et al*., P-selectin and P-selectin glycoprotein ligand 1 are major determinants for Th1 cell recruitment to nonlymphoid effector sites in the intestinal lamina propria. *J. Exp. Med.* **198**, 369–377 (2003).
8. K. M. Veerman *et al*., Interaction of the selectin ligand PSGL-1 with chemokines CCL21 and CCL19 facilitates efficient homing of T cells to secondary lymphoid organs. *Nat. Immunol.* **8**, 532–539 (2007).
9. J. G. Fox, Z. Ge, M. T. Whary, S. E. Erdman, B. H. Horwitz, Helicobacter hepaticus infection in mice: Models for understanding lower bowel inflammation and cancer. *Mucosal Immunol.* **4**, 22–30 (2011).
10. J. G. Fox, The non-H pylori helicobacters: Their expanding role in gastrointestinal and systemic diseases. *Gut* **50**, 273–283 (2002).
11. J. G. Fox, T. C. Wang, Inflammation, atrophy, and gastric cancer. *J. Clin. Invest.* **117**, 60–69 (2007).
12. J. N. Chai *et al*., *Helicobacter* species are potent drivers of colonic T cell responses in homeostasis and inflammation. *Sci. Immunol.* **2**, eaal5068 (2017).
13. K. J. Maloy *et al*., CD4+CD25+ T(R) cells suppress innate immune pathology through cytokine-dependent mechanisms. *J. Exp. Med.* **197**, 111–119 (2003).
14. S. Buonocore *et al*., Innate lymphoid cells drive interleukin-23-dependent innate intestinal pathology. *Nature* **464**, 1371–1375 (2010).
15. M. Coccia *et al*., IL-1β mediates chronic intestinal inflammation by promoting the accumulation of IL-17A secreting innate lymphoid cells and CD4(+) Th17 cells. *J. Exp. Med.* **209**, 1595–1609 (2012).
16. C. Pearson *et al*., ILC3 GM-CSF production and mobilisation orchestrate acute intestinal inflammation. *eLife* **5**, e10066 (2016).
17. N. Powell *et al*., The transcription factor T-bet regulates intestinal inflammation mediated by interleukin-7 receptor+ innate lymphoid cells. *Immunity* **37**, 674–684 (2012).
18. C. S. Klose *et al*., A T-bet gradient controls the fate and function of CCR6-RORγt+ innate lymphoid cells. *Nature* **494**, 261–265 (2013).
19. L. C. Rankin *et al*., The transcription factor T-bet is essential for the development of NKp46+ innate lymphocytes via the Notch pathway. *Nat. Immunol.* **14**, 389–395 (2013).
20. G. Sciumé *et al*., Distinct requirements for T-bet in gut innate lymphoid cells. *J. Exp. Med.* **209**, 2331–2338 (2012).
21. S. Li *et al*., Aryl hydrocarbon receptor signaling cell intrinsically inhibits intestinal group 2 innate lymphoid cell function. *Immunity* **49**, 915–928.e5 (2018).
22. J. H. Bernink *et al*., Interleukin-12 and -23 control plasticity of CD127(+) group 1 and group 3 innate lymphoid cells in the intestinal lamina propria. *Immunity* **43**, 146–160 (2015).
23. C. Vonarbourg *et al*., Regulated expression of nuclear receptor RORγt confers distinct functional fates to NK cell receptor-expressing RORγt(+) innate lymphocytes. *Immunity* **33**, 736–751 (2010).
24. M. L. Robinette *et al*., IL-15 sustains IL-7R-independent ILC2 and ILC3 development. *Nat. Commun.* **8**, 14601 (2017).
25. S. Sawa *et al*., RORγt+ innate lymphoid cells regulate intestinal homeostasis by integrating negative signals from the symbiotic microbiota. *Nat. Immunol.* **12**, 320–326 (2011).
26. E. A. Kiss *et al*., Natural aryl hydrocarbon receptor ligands control organogenesis of intestinal lymphoid follicles. *Science* **334**, 1561–1565 (2011).
27. J. S. Lee *et al*., AHR drives the development of gut ILC22 cells and postnatal lymphoid tissues via pathways dependent on and independent of Notch. *Nat. Immunol.* **13**, 144–151 (2011).
28. J. Qiu *et al*., The aryl hydrocarbon receptor regulates gut immunity through modulation of innate lymphoid cells. *Immunity* **36**, 92–104 (2012).
29. J. U. Scher *et al*., Expansion of intestinal Prevotella copri correlates with enhanced susceptibility to arthritis. *eLife* **2**, e01202 (2013).
30. M. G. Rooks *et al*., Gut microbiome composition and function in experimental colitis during active disease and treatment-induced remission. *ISME J.* **8**, 1403–1417 (2014).
31. R. Caruso *et al*., A specific gene-microbe interaction drives the development of Crohn's disease-like colitis in mice. *Sci. Immunol.* **4**, eaaw4341 (2019).
32. C. L. Franklin *et al*., Enteric lesions in SCID mice infected with "Helicobacter typhlonicus," a novel urease-negative Helicobacter species. *Lab. Anim. Sci.* **49**, 496–505 (1999).
33. J. G. Fox *et al*., A novel urease-negative Helicobacter species associated with colitis and typhlitis in IL-10-deficient mice. *Infect. Immun.* **67**, 1757–1762 (1999).
34. J. W. Collins *et al*., Citrobacter rodentium: Infection, inflammation and the microbiota. *Nat. Rev. Microbiol.* **12**, 612–623 (2014).
35. K. Sugimoto *et al*., IL-22 ameliorates intestinal inflammation in a mouse model of ulcerative colitis. *J. Clin. Invest.* **118**, 534–544 (2008).
36. H. Araoka *et al*., Risk factors for recurrent Helicobacter cinaedi bacteremia and the efficacy of selective digestive decontamination with kanamycin to prevent recurrence. *Clin. Infect. Dis.* **67**, 573–578 (2018).
37. Y. Fujiya *et al*., Successful treatment of recurrent *Helicobacter fennelliae* bacteraemia by selective digestive decontamination with kanamycin in a lung cancer patient receiving chemotherapy. *JMM Case Rep.* **3**, e005069 (2016).
38. Z. Ge *et al*., Helicobacter hepaticus cytolethal distending toxin promotes intestinal carcinogenesis in 129Rag2-deficient mice. *Cell. Microbiol.* **19**, e12728 (2017).
39. F. Melo-Gonzalez *et al*., Antigen-presenting ILC3 regulate T cell-dependent IgA responses to colonic mucosal bacteria. *J. Exp. Med.* **216**, 728–742 (2019).
40. J. Kim *et al*., Complete genome sequencing and comparative genomic analysis of *Helicobacter Apodemus* isolated from the wild Korean striped field mouse *(Apodemus agrarius*) for potential pathogenicity. *Front. Pharmacol.* **9**, 838 (2018).
41. J. Frank *et al*., The complete genome sequence of the murine pathobiont Helicobacter typhlonius. *Front. Microbiol.* **6**, 1549 (2016).